NONLINEAR HYDRODYNAMIC PRESSURES ON RIGID ARCH DAMS DURING EARTHQUAKES

Bang-Fuh CHEN[1] And Yin-Sen YUAN[2]

SUMMARY

A complete three-dimensional finite difference scheme has been developed and used to analyze the nonlinear hydrodynamic pressures on rigid arch dam during earthquakes. Not only the free surface waves but also the nonlinear convective acceleration were included in the analysis. Various dam shapes and reservoir banks were studied and the characteristic of nonlinear contribution due to curved geometry and free surface waves were discussed. Numerical experiments have been made to determine the desirable mesh size arrangements and time increments. The computational accuracy were assured by checking both mass and momentum balance at each time step. Different open boundary treatments were used and compared. The present open boundary treatment is highly recommended for numerical study of unbounded fluid dynamic problems. Under Kobe earthquake, the possible peak rise of water surface could be as large as 18 meters for an arch dam with water depth of 100 meters. This huge water surface rise would cause sever hazards to human and hydraulic structures.

INTRODUCTION

The calculation of hydrodynamic pressures acting on dam faces during earthquakes is important to the analysis and design of a dam. The first rigorous hydrodynamic analysis of the dam-reservoir system was made by Westergaard in 1933. In the followed six decades, extensive analyses were performed by many researchers. The typical contributors include Chopra and his co-workers (1967, 1981) for interactions among reservoir, dam and foundation; Lee and Tsai (1991) for reporting different approaches and presenting an artificial upstream radiation condition; Chwang (1978) and Liu (1986), respectively, for the exact solutions of hydrodynamic pressures on inclined dam faces with horizontal and inclined reservoir bottoms. All the above analyses were based on the assumption of water remaining horizontal during earthquakes, and this assumption was valid when the instantaneous ground displacement was small. The rise of the free surface and the nonlinear convective acceleration were first included in Chwang's (1983) analysis with a rigid vertical wall and a constant ground acceleration. Chen (1990, 1994,1996,1999), using finite difference scheme, comprehensively studied the variation of the water surface and the corresponding nonlinear hydrodynamic pressures acting on rigid (or deformable) dam faces with various reservoir shapes. After aforementioned studies, the effects of interaction among dam, reservoir and foundation were shown to be significant on hydrodynamic pressures. The free surface wave could increase hydrodynamic pressures. The rise of the water surface may cause damage to boats, hydraulic structures and human safety in the recreational areas.

Almost all of the aforementioned analyses were limited to the two dimensional analyses. Using three dimensional potential flow theory, Rashed and Iwan (1984) studied hydrodynamic pressure on a short-length rigid gravity dam with a rectangular reservoir (i.e., vertical banks and horizontal reservoir bottom). Wang and Hung (1990) reported the nonlinear hydrodynamic pressures on vertical dam faces associated also with a rectangular reservoir. Almost all the other three dimensional analyses of dam hydrodynamics were for arch dams. Same as the two-dimensional problems, all the three-dimensional analyses for arch dam hydrodynamics were linear analyses, that is, not only free surface waves but also nonlinear convective acceleration were

[1] Professo Department of Marine Environment, National Sun Yat-sen University, Kaohsiung, Taiwan
[2] Formerly graduate student Department of Marine Environment, National Sun Yat-sen University, Kaohsiung, Taiwan

neglected in those analyses. The curved geometric shape of the arch dam face may augment the nonlinear effect of convective acceleration on hydrodynamic pressure. The rise of water surface on arch dam face may larger than that on a vertical rectangular gravity dam because of the more complicate geometric effect. Therefore, the nonlinear hydrodynamic effects on arch dam hydrodynamics would be more significant than those on concrete gravity dam. A finite difference method associated with coordinates transformation were used in the present nonlinear analysis of arch dam hydrodynamics. Not only the free surface waves but also the nonlinear convective acceleration were included in the analysis. Various dam shapes and reservoir banks were studied. The characteristic of nonlinear contribution due to curved geometry and free surface waves were discussed. Different open boundary treatments were used and compared.

BASIC EQUATIONS

For an invicid fluid, the three-dimensional equations of motion of fluid in Cartesian coordinate systems can be written as following

$$\frac{\partial u}{\partial t} + u\frac{\partial u}{\partial x} + v\frac{\partial u}{\partial y} + w\frac{\partial u}{\partial z} = -\frac{1}{\rho}\frac{\partial p}{\partial x} \tag{1}$$

$$\frac{\partial v}{\partial t} + u\frac{\partial v}{\partial x} + v\frac{\partial v}{\partial y} + w\frac{\partial v}{\partial z} = -\frac{1}{\rho}\frac{\partial p}{\partial y} \tag{2}$$

$$\frac{\partial w}{\partial t} + u\frac{\partial w}{\partial x} + v\frac{\partial w}{\partial y} + w\frac{\partial w}{\partial z} = -g - \frac{1}{\rho}\frac{\partial p}{\partial z} \tag{2}$$

$$P = P_d + P_s = P_d - \rho gy \tag{3}$$

where u, v and w are, respectively, the velocity components of fluid in the x-, y- and z- directions, , p the pressure, ρ the fluid density and g the gravitational acceleration. The continuity equation for the incompressible flow can be written as

$$\frac{\partial u}{\partial x} + \frac{\partial v}{\partial y} + \frac{\partial w}{\partial z} = 0 \tag{4}$$

The water depth, h(x,t), can be solved with the other three unknowns (p, u, v and w) from the kinematic boundary condition on the free surface. That is

$$\frac{\partial h}{\partial t} + u\frac{\partial h}{\partial x} + v\frac{\partial h}{\partial y} = w \qquad at \qquad Z = h - d_0 \tag{5}$$

Taking partial differentiation of equations (1) and (2) with respective to x and z and summing up the results, one can obtain

$$\nabla^2 p = -\rho\frac{\partial}{\partial x}\left(u\frac{\partial u}{\partial x} + v\frac{\partial u}{\partial y} + w\frac{\partial u}{\partial z}\right) - \rho\frac{\partial}{\partial z}\left(u\frac{\partial v}{\partial x} + v\frac{\partial v}{\partial y} + w\frac{\partial v}{\partial z}\right) - \rho\frac{\partial}{\partial z}\left(u\frac{\partial w}{\partial x} + v\frac{\partial w}{\partial y} + w\frac{\partial w}{\partial z}\right)$$

An irregular tank wall face and tank bottom can be mapped onto a rectangular one by the proper coordinate transformations (Chen et al., 1999),one can map any shape of left tank wall to x*=0, and upstream end to x*=1, the free surface to z*=0, reservoir bottom to z*=1 and both reservoir banks to y*=0 and y*=1. The main advantage of these transformations is to map a non-rectangular and time dependent flow field onto a time-independent rectangular domain. In this case, all the time-dependent geometric and dynamic boundary conditions are cast in the equations of motion along with the ground acceleration. The difference equations for space derivatives are using central difference approximation, and are using forward or backward difference approximation when they reach the boundaries. The difference equations for time derivatives are also using central difference approximation. The detail expressions can be found in Chen et al. 1999 and are omitted in the manuscript.

RESULTS AND DISCUSSIONS

In the present study, various dam shapes and reservoir banks are used as examples. Their definition sketches are shown in Fig. 1. with brief descriptions as follow:

Type A: flat dam face, parallel reservoir banks; width of reservoir is twice as large as water depth,
   i.e. $b_4-b_3=2d_0$.
Type B: circular arch dam face, parallel reservoir banks, $b_4-b_3=2d_0$
Type C: circular arch dam face, reservoir banks have two parts. The first part inclines to dam face
   with an angle φ and the second part is parallel to each other and $b_4-b_3=4d_0$.

The dimensionless ground displacement, ε^2, is defined as the ratio of the ground displacement to the undisturbed water depth. The hydrodynamic force coefficient is calculated by normalizing the integral of the hydrodynamic pressure along the dam face by $\rho g d_0^2$, i.e. $C_F = \int p/\rho g d_0^2$. At t = 0.0001 second, $a_x = 0.5g$ and $d_0^2=100m$, $\varepsilon^2 = 2.45 \times 10^{-10}$ and the water surface variation is so small that the corresponding hydrodynamic pressure will be referred as the onset hydrodynamic pressure.

Type A system is a special case of Type B whose radius of curvature is approaching to infinity. With the assumption of invicid fluid, three dimensional analysis of type A system exciting only by a_x can actually be simplified by a two dimensional analysis. Fig. 2 presents the onset hydrodynamic pressure along dam face due to $a_x=0.5g$ ground acceleration. Also shown in the figure are results of Wang and Hung (1990), indicated by solid circle, and a two-dimensional analysis by Chen (1994), by hollow circle. As reported in the figure, the result by present three-dimensional analysis is identical with author's previous two-dimensional analysis and a little bit smaller than that of Wang and Hung (1990).

Due to $a_x=0.5g$ ground exciting and for type B system, Fig. 3 shows the onset hydrodynamic pressure, at toe of dam, across arch dam face with various radius of curvature (R) of the arch dam face. As presented in the figure, the larger the radius of curvature is, the smaller (larger) the hydrodynamic pressure at abutment (crown) will be, and the pressures at crown and abutments will be equal to that of type A system when R is approaching to infinity.

All the aforementioned results are due to a horizontal ground exciting only. For a complete three-dimensional analysis, simultaneous action of three components ground acceleration should be included in the analysis. However, the vertical ground acceleration is, in general, just a change of acceleration of gravity. Fig. 4 presents the onset hydrodynamic pressure along arch dam face for various radius of curvature R and an equivalent hydrostatic pressure distribution is found. For a constant ground acceleration a=0.5g with arbitrary exciting directions, Fig. 5 shows the onset hydrodynamic pressure distribution at toes of crown, left and right abutments versus various exciting directions. The parameter α is defined as the angle between exciting direction and positive x-direction. As listed in the figure, the maximum pressure does not always occur when $a=a_x$ only and a complete three-dimensional analysis should be considered in the analysis and design of the arch dam structures. For a rigid arch dam motion with type B system, the onset hydrodynamic force coefficients on arch dam face can be related to the intensity of ground accelerations by a simple formula

$$C_F = Cx\ a_x + 0.5\ a_y + Cz\ a_z$$

where Cx and Cz are functions of radius of curvature and location of arch dam and their relationships are reported in Figs. 6 and 7. At crown, Cx has smallest value and Cz = 0. All the results are the onset hydrodynamic pressures. In order to discuss the nonlinear effects, the 0.5g constant ground acceleration is prolonged to one second. For type B system, Fig. 8 shows the rising of the water surface along x-axis (crown) and reservoir banks. At the dam face has the maximum rise and the rise becomes nil when $x^*=0.4$ or $x=1.6d_0$. The rise of water surface along x-axis increases as R does. On the contrary, the rise of water surface along reservoir banks decreases as R increases. At $\varepsilon^2=0.02$ and $R=1.2d_0$ and $d_0=100m$, the maximum surface rise could be as large as 6.5 m at both abutments and 6m at crown. The significant rise of water surface may cause overflow and damage to hydraulic structures and human safety in recreational area.

To discuss the effects of free surface waves and nonlinear convective acceleration on hydrodynamic pressures, the following four cases were studied and compared.

1. Neglect both free surface and convective acceleration effects
2. neglect free surface effect but consider convective acceleration effect.
3. consider free surface effect but neglect convective acceleration effect.
4. consider both free surface and convective acceleration effects.

At $\varepsilon^2 = 0.02$, Fig. 9 presents the distribution of hydrodynamic pressure, at toe of dam of type B system with $R = 1.5 d_0$, across the arch dam face for the above four cases. As shown in the figure, the free surface effect and convective acceleration effect on hydrodynamic pressures are about the same. And both combined effects will augment hydrodynamic pressures to 10% larger than those of a linear analysis. The arch dam excited by a real record earthquake, El-Centro earthquake Oct. 15, 1979, was also analyzed. Both nonlinear (case IV) and linear analyses (case I) were made and compared. For type B system and $R = 1.5 d_0$, Fig. 10 shows the time histories (t = 5.5 - 7.5sec.) of hydrodynamic force coefficients at crown and both abutments respectively. Also plotted in these figures are the results by a linear analysis (dotted line). The maximum difference between both analyses is about 10%. The time histories of the rise of the water surface at crown and both abutments are shown in Fig. 11. As shown in the figure, the shapes of three curves are similar. Although there is no simple formula can relate the rise of water surface to the ground displacement, the rise of water surface is primary dominated by the pronounced ground displacement.

CONCLUSIONS

The geometry of the reservoir shapes has significant influence on hydrodynamic pressures on dam face. For type A reservoir system, the three-dimensional analysis can be simplified as a two dimensional analysis if the exciting acceleration is in longitudinal direction, i.e. in x-direction. For type B system, the dam face is a circular arc. The larger the radius of curvature is, the smaller (larger) the hydrodynamic pressure at abutment (crown) will be. For type C system, similar behavior of type B system exists. While for $R = d_0$, dam width $= 2d_0$ and $b_3 - b_4 = 4d_0$, the arch dam motion is more like a circular cylinder motion, the distribution of hydrodynamic pressure across dam face has a lifting at crown but that behavior would not occur for arch dam with larger radius of curvature. For arbitrary exciting direction, the maximum hydrodynamic pressure is affected by the simultaneous actions of three ground components. And a complete three-dimensional analysis should be considered in the analysis of the arch dam structures. Due to a rigid dam motion, the onset hydrodynamic force coefficients on dam face can be related to the intensity of ground acceleration by a simple formula $C_F = Cx\ a_x + 0.5\ a_y + Cz\ a_z$. The effects of surface wave and nonlinear convective acceleration on hydrodynamic pressure are about the same. Both effects could augment the hydrodynamic pressure to 10% larger than that of a linear analysis. Due to El-Centro Oct. 1979 earthquakes (the peak ground displacement = 0.8 meter), the maximum rise of the water surface at abutment of type B system is about 3.5 meters. The recent Kobe earthquake has a peak ground displacement as large as 4 meters. Thus, under Kobe earthquake, the possible peak rise of the water surface could be larger than 18 meters. This huge rise of water surface would cause severe damage to hydraulic structures, human safety in recreational area and even cause overflow to affect the safety of the arch dam.

REFERENCE:

Chen, B. F., (1994), "Nonlinear hydrodynamic pressure on dam faces with arbitrary reservoir shapes," J. of Hydra Res., 32(3), 401-413.

Chen, B. F., (1996), "Nonlinear hydrodynamic effects on concrete dam", Engrg. Str., 18 (3), pp. 201-212.

Chen, B. F., Yuan, Y.S. and Lee, J.F.(1999)," Three-dimensional nonlinear hydrodynamic pressures by earthquakes on dam faces with arbitrary reservoir shapes", J. Hydra. Res., 37(2), 163-187.

Chopra, A.K., (1967), "Hydrodynamic pressures on dams during earthquakes," J. Engrg Mech. Div., ASCE, 93, 205-223.

Chopra, A. K. and Gupta, S., (1981), "Hydrodynamic and foundation interaction effects in earthquake response of a concrete gravity dam," J. Struct. Div., ASCE, Vol. 107, 1399-1412.

Chwang, A. T., (1978), "Hydrodynamic pressures on sloping dams during earthquakes: Part 2, Exact Theory," J. Fluid Mech., 87, 342-348.

Chwang, A. T., (1983), "Nonlinear hydrodynamic pressure on an accelerating plate," J. Physics Fluids, 26(2), 383-387.

Hung, T. K. and Wang, M. H., (1987), "Nonlinear hydrodynamic pressure on rigid dam motion," J. Engrg. Mech., 113(4), 482-499.

Hung, T. K. and Chen, B. F., (1990), "Nonlinear hydrodynamic pressure on dams," J. Engrg. Mech., 116(6), 1372-1391.

Liu, P. L.-F., (1986), "Hydrodynamic pressure on rigid dams during earthquakes', J. Fluid Mech., 165, 131-145.

Rashed, A. A. and Iwan, W. D., (1984), "Hydrodynamic pressure on short-length gravity dams", J. Engrg. Mech., 110(9), 1264-1283.

Lee, G. C. and Tsai, C. S., (1991), "Time-domain analysis of dam-reservoir system, I: exact solution", J. Engrg. Mech., 117(9), pp. 1990-2006.

Wang, M. H. and Hung, T. K., (1990), "Three dimensional analysis of pressure on dams," J. Engrg. Mech., 116(6), 1290-1304.

Westergaard, H. M., (1933), "Water pressure on dams during earthquakes," Trans. ASCE 98, 418-472.
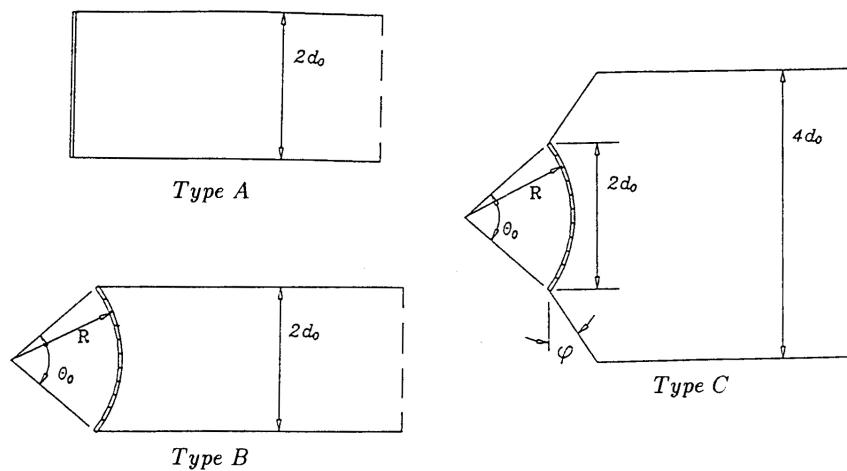
Fig.1. The top-view of various reservoir system
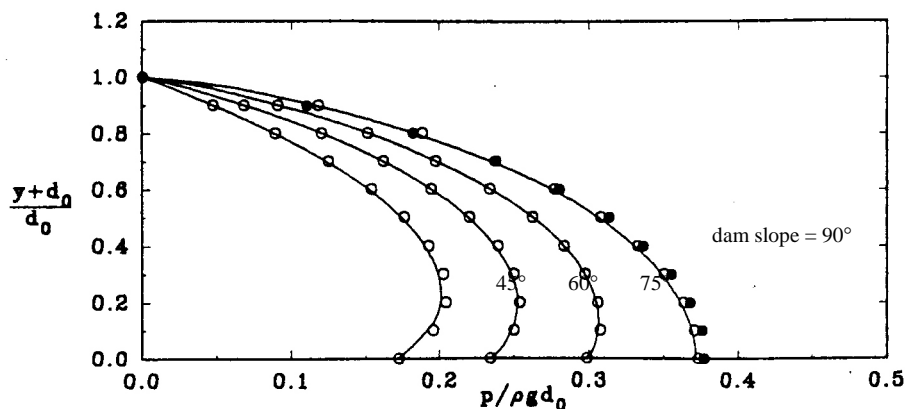
Fig.2. The onset hydrodynamic pressures along dam face for Type A system with $a_x=0.5g$, line: present 3D analysis, hollow circle: author's 2D analysis, solid circle: Wang and Hung.
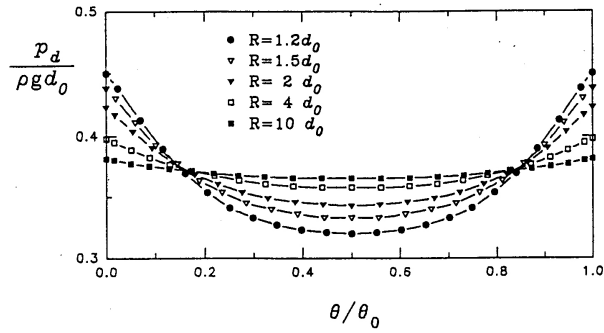
Fig.3 The distribution of onset hydrodynamic pressures, at toe, across dam face for type B system, a_x=0.5g and various radius of curvatures.
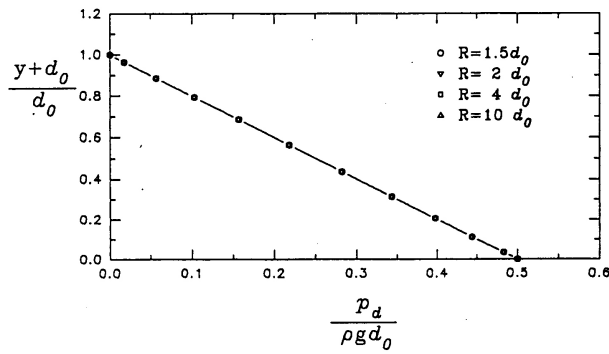
Fig.4. The distribution of onset hydrodynamic pressure along dam face for type B system, a_y=0.5g, and various R.
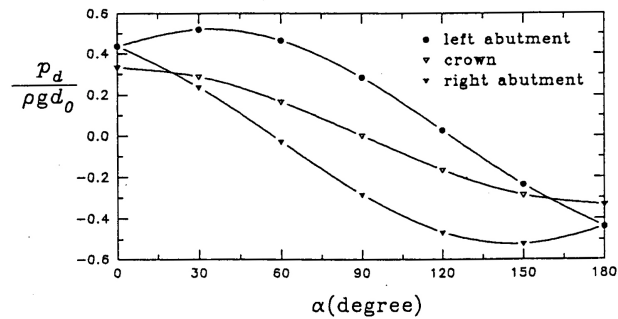

Fig.5. For type B system, due to different orientation of 0.5g horizontal ground acceleration, the variation of hydrodynamic pressure at toe of both abutment and crown.
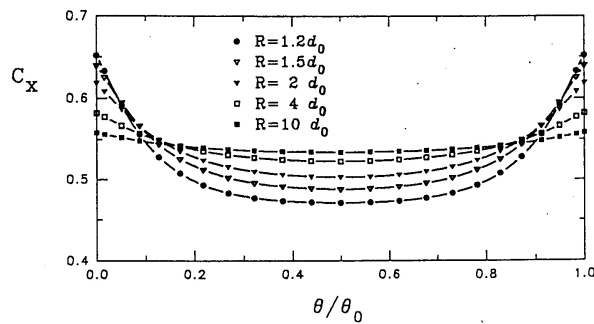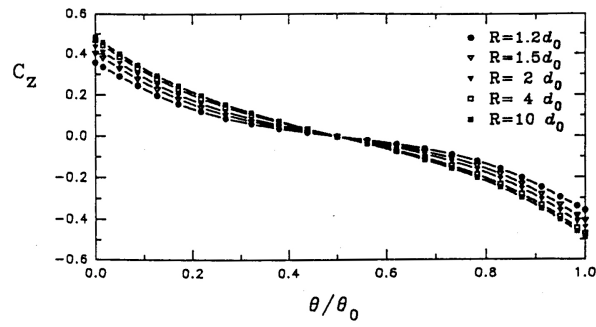

Fig.6. For type B system, C_x versus radius of curvatures

Fig.7. For type B system, C_x versus radius of curvatures
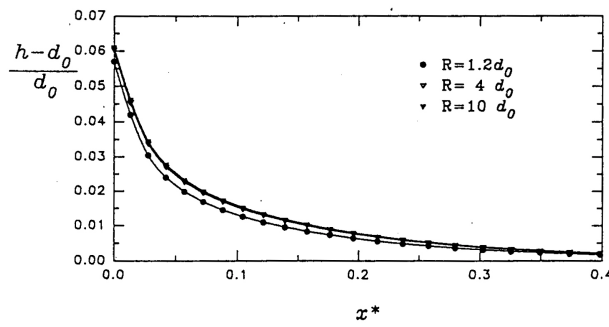
Fig.8. For type B system and $!^2$=0.02, the rise of the water surface along x-axis

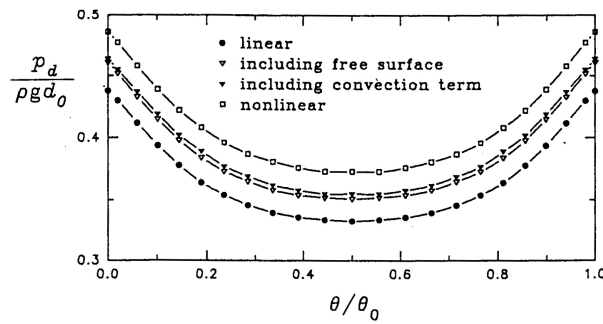**Fig.9. For type B system , R=1.5$d_0$and $!^2$=0.02, comparison of the distribution of hydrodynamic pressures at toe across dam face for linear, partial nonlinear and complete nonlinear analysis.**
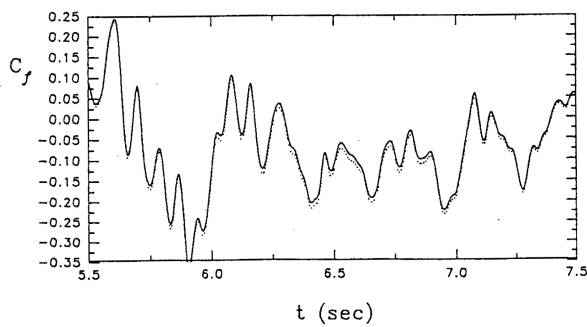

Fig.10. The comparison of hydrodynamic force coefficient at abutment of linear (dash line) and nonlinear (solid line) analysis, due to El-Centro earthquakes, Oct. 15,1979.
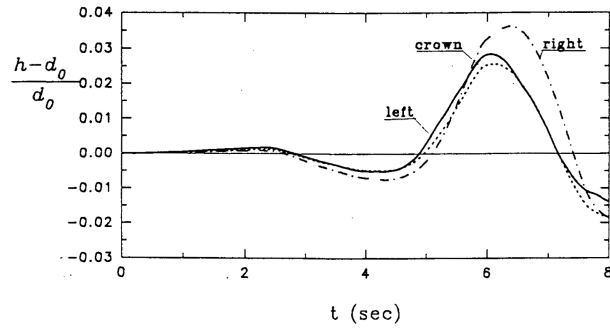
7

Fig.11. For type B system, the time histories of rise of surface at reservoir banks and crown, due to El-Centro earthquakes, Oct. 15, 1979.
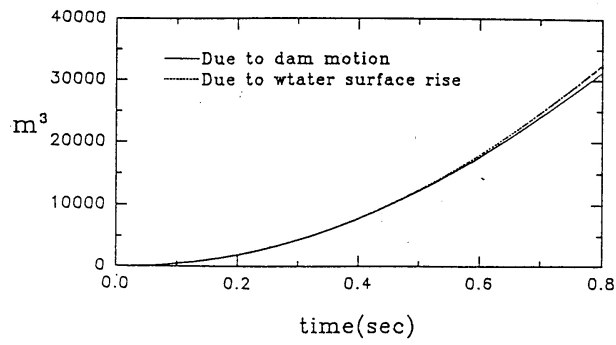

Fig.12. For type B system and d_0=100m, the comparison of the volume of water surface rise and that of the dam motion